

Numerical Simulations of the SEIR Epidemiological Model with Population Heterogeneity to Assess the Efficiency of Social Isolation in Controlling COVID-19 in Brazil

A. L. O. SOARES^{1*}, C. M. CALOI² and R. C. BASSANEZI³

Received on July 31, 2020 / Accepted on October 1, 2021

ABSTRACT. On 30 January 2020, the World Health Organization (WHO) officially declared the epidemic of Coronavirus (COVID-19), which is a highly contagious virus that has been causing deaths worldwide. Early treatment was proven to be inefficient and social isolation became the main factor inhibiting the disease, before vaccination. In this article, we evaluate the efficiency of this isolation as a control, through numerical simulations of mathematical model of the SEIR type (Susceptible-Exposed-Infectious-Removed) with population heterogeneity, in which the susceptible population was distributed according to the age group (children / youth, adults and elderly) and the infectious population was categorized according to the severity of symptoms (severe, mild and asymptomatic). The results suggest that the isolation of only one of the susceptible subpopulations is inefficient to control the spread of the virus, which indicates that vertical isolation is not enough to contain the proliferation of COVID-19. Furthermore, the disease does not have the strength to invade the population when there is sufficient social isolation composed of susceptible subpopulations and the epidemiological scenario improves when there is awareness of the importance of the quarantine of infectious individuals with mild symptoms.

Keywords: epidemiological modeling, social Isolation, COVID-19.

1 INTRODUCTION

On 12 December 2019, several cases of pneumonia occurred in Wuhan, China, that were caused by an identified β -coronavirus, which was named COVID-19 by the World Health Organization (WHO) and SARS-CoV-2 by the International Committee of Coronavirus Study [5]. On 1 March 2020, China had a total of 79.968 cases of COVID-19, including 2.873 deaths. After a year, in

*Corresponding author: Anna Oenning Soares – E-mail: ligiaoenning@gmail.com

¹Departamento de Matemática, ICET, Universidade Federal de Mato Grosso, Av. Fernando Corrêa da Costa, 2367, 78060-900 Cuiabá, MT, Brazil – E-mail: ligiaoenning@gmail.com <https://orcid.org/0000-0002-6076-2037>

²ICEC, Instituto Cuiabá de Ensino e Cultura, Rua Osvaldo da Silva Corrêa, 621, 78048-005 Cuiabá, MT, Brazil – E-mail: carolinecaloi@gmail.com <https://orcid.org/0000-0003-4201-8594>

³Departamento de Matemática Aplicada, IMECC, Universidade Estadual de Campinas, Rua Sérgio Buarque de Holanda, 651, 13083-859 Campinas, SP, Brazil – E-mail: rodneyb@unicamp.br <https://orcid.org/0000-0002-5219-5319>

May 2021, China registered about 102.000 cases and 4.846 deaths from COVID-19 [2, 14], which were much lower numbers compared to most countries.

Knowing that the virus was highly transmissible and that it was being spread mainly through the respiratory tract, through droplets and respiratory secretions [8] and that the incubation period is from 1 to 14 days, being contagious during the latency period, from 3 to 7 days [6], drastic measures to limit human mobility and isolate suspected cases were implemented in China. These measures successfully reduced the transmission of COVID-19 [7].

The epidemic has since spread around the world and according to the Ministry of Health, the first case of COVID-19 in Brazil occurred on 26 February 2020, through a 61-year-old man, who was resident in São Paulo, who had travelled to Italy and returned to Brazil on 21 February. By the end of March of that same year, Brazil had already registered approximately 4.000 active cases and 140 deaths and after a little more than a year, in May 2021, Brazil had registered 14.930.183 cases and 414.339 deaths by COVID-19 [10, 11].

Shaman et al. (2020) [9] used a mathematical model to simulate the spatiotemporal dynamics of SARS-CoV-2 infections among 375 Chinese cities, with the aim of verifying the endemic potential of the virus. They concluded that 86% of infections occur through undocumented infections, which we can consider to be people who did not manifest symptoms or manifested mild symptoms. In their study, they showed the importance of infectious individuals with mild and asymptomatic symptoms in the dynamics of COVID-19 transmission.

We propose a mathematical model for a case study of Covid-19 in Brazil in which the infectious population is categorized according to the severity of symptoms, which are asymptomatic, mild symptomatic and severe symptomatic. Using the process of numerical simulations, with baseline data of the pandemic in Brazil, we sought to evaluate the effect of isolation in the pandemic considering the susceptible population divided into three categories, according to their age group.

2 EPIDEMIOLOGICAL MODELING

In this section, we present the epidemiological modeling of the dynamics of COVID-19 propagation. Therefore, we will discuss some important points in the dynamics of transmission of the virus that causes COVID-19 and measures to prevent the transmission of the virus.

The virus that causes COVID-19 can be transmitted in the pre-symptomatic phase. This phase comprises a period in which the organism is already contaminated by the virus but still does not present symptoms. This phase is also known as latent and individuals are classified as exposed or latent. Researchers have also shown that asymptomatic and infectious individuals with mild symptoms contribute to the dynamics of transmission of this disease [1, 9].

To control the spread of the virus, the WHO suggested preventive measures such as the use of a protective mask, basic hygiene care, and social isolation, among others [13]. In Brazil, partial measures were adopted, such as the suspension of in-person classes in schools and universities,

mostly affecting the mobility of children and young people. In addition, some jobs were moved to the home office modality, mainly affecting adults [3, 12].

Given the above, we propose an epidemiological model based on the SEIR (Susceptible-Exposed-Infectious-Removed) model with population heterogeneity, in which the susceptible population differs by age group—being children/young people (S_1), adults (S_2) and elderly (S_3)—and the infectious population was categorized according to the severity of symptoms—being severe symptomatic (I_1), mild symptomatic (I_2) and asymptomatic (I_3). In addition, the pre-symptomatic phase (E) is considered, in which individuals already infected but not yet showing symptoms can transmit the virus, and individuals recovered and dead disease are accounted for in the Removed compartment (R). The transfer diagram in Figure 1 illustrates the structure of the model.

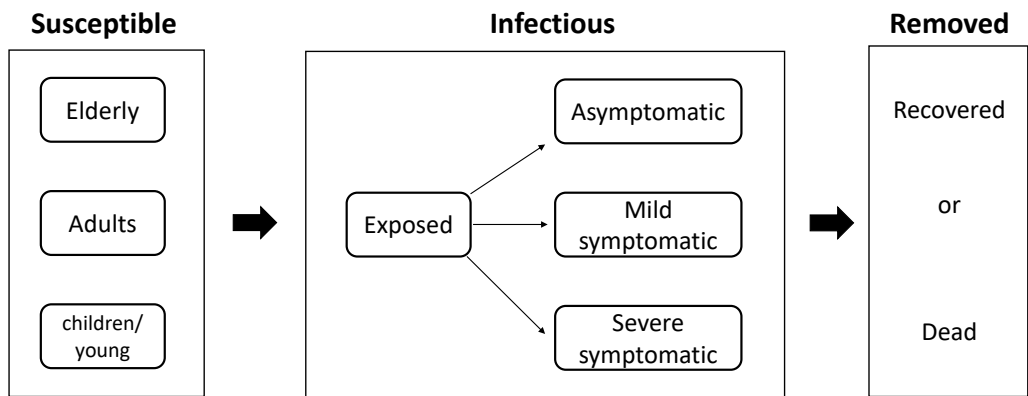


Figure 1: Transfer diagram of the COVID-19 model.

Considering the classical law of mass action in an homogeneously mixed population, the mathematical model of COVID-19 propagation is given by a system of nonlinear autonomous differential equations:

$$\left\{ \begin{array}{l}
 \frac{dS_1}{dt} = - \left(\varepsilon\beta E + \sum_{i=1}^3 \varepsilon_i\beta_i I_i \right) (1 - \rho_1) \frac{S_1}{N} \\
 \frac{dS_2}{dt} = - \left(\varepsilon\beta E + \sum_{i=1}^3 \varepsilon_i\beta_i I_i \right) (1 - \rho_2) \frac{S_2}{N} \\
 \frac{dS_3}{dt} = - \left(\varepsilon\beta E + \sum_{i=1}^3 \varepsilon_i\beta_i I_i \right) (1 - \rho_3) \frac{S_3}{N} \\
 \frac{dE}{dt} = \left(\varepsilon\beta E + \sum_{i=1}^3 \varepsilon_i\beta_i I_i \right) \frac{\sum_{i=1}^3 (1 - \rho_i) S_i}{N} - \gamma E \\
 \frac{dI_1}{dt} = \alpha\gamma E - (\sigma + \mu) I_1 \\
 \frac{dI_2}{dt} = \frac{(1 - \alpha)}{2} \gamma E - \sigma I_2 \\
 \frac{dI_3}{dt} = \frac{(1 - \alpha)}{2} \gamma E - \sigma I_3 \\
 \frac{dR}{dt} = \sigma \left(\sum_{i=1}^3 I_i \right) + \mu I_1 \\
 S_i(0) = S_{0i}, \quad i = 1, 2, 3, \quad E(0) = E_0, \quad I_i(0) = I_{0i} \quad i = 1, 2, 3, \quad R(0) = R_0
 \end{array} \right. \tag{2.1}$$

where the parameters β , ε , ρ , γ^{-1} , σ^{-1} , μ and α represent, respectively, the force of infection, fraction of non-isolated infectious, fraction of isolated susceptible, mean latent period, mean infectious period, mean lethality of the disease and fraction of exposed individuals who progress to severe symptoms.

Note that the total population (N) is constant because the sum of the system equations (2.1) is zero. Furthermore, the removed individuals do not interfere in the dynamics of the other subpopulations. Thus, when the variables S_1 , S_2 , S_3 , E , I_1 , I_2 , I_3 are known, the removed individuals can be obtained by,

$$R(t) = N - (S_1(t) + S_2(t) + S_3(t) + E(t) + I_1(t) + I_2(t) + I_3(t)). \tag{2.2}$$

For qualitative analysis of the model 2.1, we will reorder the system equations to adapt the theory involving the calculation of the basic reproduction number of the disease presented by Driessche and Watmough (2002) [4], and the removed are given by equation (2.2).

Reordering the system 2.1 becomes,

$$\begin{cases} E' = \left(\varepsilon\beta E + \sum_{i=1}^3 \varepsilon_i\beta_i I_i \right) \frac{\sum_{i=1}^3 (1-\rho_i)S_i}{N} - \gamma E \\ I'_1 = \alpha\gamma E - (\sigma + \mu)I_1 \\ I'_2 = \frac{(1-\alpha)}{2}\gamma E - \sigma I_2 \\ I'_3 = \frac{(1-\alpha)}{2}\gamma E - \sigma I_3 \\ S'_1 = - \left(\varepsilon\beta E + \sum_{i=1}^3 \varepsilon_i\beta_i I_i \right) (1-\rho_1) \frac{S_1}{N} \\ S'_2 = - \left(\varepsilon\beta E + \sum_{i=1}^3 \varepsilon_i\beta_i I_i \right) (1-\rho_2) \frac{S_2}{N} \\ S'_3 = - \left(\varepsilon\beta E + \sum_{i=1}^3 \varepsilon_i\beta_i I_i \right) (1-\rho_3) \frac{S_3}{N} \end{cases} \tag{2.3}$$

The system 2.3 takes the form

$$x' = f(x)$$

where $x = (E, I_1, I_2, I_3, S_1, S_2, S_3)$ is the state variable and $f : \mathbb{R}^7 \rightarrow \mathbb{R}^7$ the function with coordinates $f = (f_1, f_2, f_3, f_4, f_5, f_6, f_7)$ where $f_1 = E'$, $f_2 = I'_1$, $f_3 = I'_2$, $f_4 = I'_3$, $f_5 = S'_1$, $f_6 = S'_2$ and $f_7 = S'_3$. Because f is of class C^∞ , the system 2.3 admits a unique solution for each initial condition $x_0 \in \mathbb{R}^7$.

The biologically feasible region or epidemiologically feasible region given by $\Omega = \left\{ (E, I_1, I_2, I_3, S_1, S_2, S_3) \in \mathbb{R}_+^7 \mid E + \sum_{i=1}^3 I_i + \sum_{i=1}^3 S_i \leq N \right\}$ is positively invariant for the system 2.3.

Moreover, the system 2.3 has an infinite number of equilibrium points given by the set $\Omega^* = \left\{ (0, 0, 0, 0, S_1^*, S_2^*, S_3^*) \in \mathbb{R}_+^7 \mid \sum_{i=1}^3 S_i^* \leq N \right\}$.

The stability of each equilibrium point will be verified by the Lyapunov Criterion. To do this, consider $x_e \in \Omega^*$ and the translation $z = x - x_e$, it follows that

$$z' = x' = f(z + x_e) \equiv f(z) \tag{2.4}$$

where $z^* = 0$ is a new system equilibrium point 2.4.

Notice that $z_i = x_i$ for $i = 1, 2, 3, 4$ and $z_{i+4} = S_i - S_i^*$ for $i = 1, 2, 3$ and consider Z the set for which z is defined and $\hat{S}_i = z_{i+4}$ for $i = 1, 2, 3$; that is, $S_i = S_i^* + \hat{S}_i$ for $i = 1, 2, 3$.

Teorema 2.1. *A Lyapunov function for system 2.4 is $L = E + \sum_{i=1}^3 I_i + \sum_{i=1}^3 (S_i^* + \hat{S}_i)$.*

Proof. In fact, $L(0) = 0$, $L(z) > 0$ for all $z \in Z \setminus \{0\}$ and

$$L'(z) = E' + \sum_{i=1}^3 I'_i + \sum_{i=1}^3 (\hat{S}'_i) = -\sigma \left(\sum_{i=1}^3 I_i + \mu I_1 \right) \leq 0$$

As $L'(z) < 0$ for $z \in Z \setminus \{0\}$ then the origin of the system is locally asymptotically stable. 2.4

□

Hence, the immediate consequence of the Theorem 2.1 is that each equilibrium point $x_e \in \Omega^*$ the system 2.3 is locally asymptotically stable. The equilibrium point $x_e \in \Omega^*$ can be called the Disease Free Equilibrium (DFE). We are now left with the problem to calculate the basic reproduction number presented by Driessche and Watmough (2002) [4].

Observe that the system 2.3 can be rewritten as

$$x' = \mathcal{F}(x) - \mathcal{V}(x)$$

where the \mathcal{F} and \mathcal{V} vector entris represent the rates of appearance of new infections and of transfer of individuals, respectively, given by

$$\mathcal{F} = \begin{bmatrix} (\varepsilon\beta E + \sum_{i=1}^3 \varepsilon_i \beta_i I_i) \left(\frac{\sum_{i=1}^3 (1-\rho_i) S_i}{N} \right) \\ 0 \\ 0 \\ 0 \end{bmatrix} \quad \text{and} \quad \mathcal{V} = \begin{bmatrix} \gamma E \\ (\sigma + \mu) I_1 - \alpha \gamma E \\ \sigma I_2 - \frac{(1-\alpha)}{2} \gamma E \\ \sigma I_3 - \frac{(1-\alpha)}{2} \gamma E \end{bmatrix}.$$

Taking $x_e \in \Omega^*$, we get the Infection Matrix $\mathbb{F} = \left. \frac{\partial \mathcal{F}}{\partial x} \right|_{x_e} = \begin{bmatrix} \varepsilon\beta\eta & \varepsilon_1\beta_1\eta & \varepsilon_2\beta_2\eta & \varepsilon_3\beta_3\eta \\ 0 & 0 & 0 & 0 \\ 0 & 0 & 0 & 0 \\ 0 & 0 & 0 & 0 \end{bmatrix}$

em que $\eta = \sum_{i=1}^3 (1-\rho_i) \frac{S_i^*}{N}$ and the Transmission Matrix $\mathbb{V} = \left. \frac{\partial \mathcal{V}}{\partial x} \right|_{x_e} =$

$$\begin{bmatrix} \gamma & 0 & 0 & 0 \\ -\alpha\gamma & \sigma + \mu & 0 & 0 \\ -\frac{1-\alpha}{2} & 0 & \sigma & 0 \\ -\frac{1-\alpha}{2} & 0 & 0 & \sigma \end{bmatrix} \quad \text{and from these we obtain the Next Generation Matrix}$$

$$\mathbb{FV}^{-1} = \begin{bmatrix} \varepsilon\beta\eta\frac{1}{\gamma} + \varepsilon_1\beta_1\eta\frac{\alpha}{\sigma+\mu} + \varepsilon_2\beta_2\eta\frac{(1-\alpha)}{2\sigma} + \varepsilon_3\beta_3\eta\frac{(1-\alpha)}{2\sigma} & \varepsilon_1\beta_1\eta\frac{\alpha}{\sigma+\mu} & \varepsilon_2\beta_2\eta\frac{1}{\sigma} & \varepsilon_3\beta_3\eta\frac{1}{\sigma} \\ 0 & 0 & 0 & 0 \\ 0 & 0 & 0 & 0 \\ 0 & 0 & 0 & 0 \end{bmatrix}.$$

According to Driessche and Watmough (2002) [4], the basic reproduction number of the disease representing the expected number of secondary cases produced by a infective individual when exposed in a completely susceptible population is given by the spectral radius of the Next Generation Matrix \mathbb{FV}^{-1} ; that is,

$$\mathcal{R}_0 = \left(\varepsilon\beta\frac{1}{\gamma} + \varepsilon_1\beta_1\frac{\alpha}{\sigma+\mu} + \varepsilon_2\beta_2\frac{(1-\alpha)}{2\sigma} + \varepsilon_3\beta_3\frac{(1-\alpha)}{2\sigma} \right) \left(\frac{\sum_{i=1}^3 (1-\rho_i) S_i^*}{N} \right). \quad (2.5)$$

Note that in expression (2.5), the fraction of susceptible individuals in social isolation and the fraction of infectious individuals circulating in society are the manipulable parameters. Thus, if

we consider the local stability of the DFE as a measure of the efficiency of disease control in the long term, then a control measure can be effective if $\mathcal{R}_0 < 1$, because this means that, on average, an infectious individual will produce less than a new infectious individual throughout their infectious period, and thus the infectious disease will not progress.

3 SIMULATIONS

Several simulations of the model (2.1) are presented in this section. By varying the parameters that represent the fractions of individuals in social isolation, we seek to evaluate the efficiency of social isolation in the propagation of COVID-19.

For the numerical simulation of the COVID-19 propagation model (2.1), we used the Matlab[®] software using the ODE45 command to solve the equations.

The initial conditions used for susceptible individuals were extracted from the Brazilian Institute of Geography and Statistics (IBGE), which estimates 59.976.963 of children/young people from 0 to 19 years old, 121.581.652 of adults between 20 and 60 years old, and 30.197.077 for seniors over 60 years old.

The parameter values of the model(2.1) were based on the parameter values presented in the article by Shaman et al. (2020) [9], as follows.

Table 1: Values for model parameters.

Parameters	Variation	Unit
β_1	0.8 to 1.5	day ⁻¹
β_2	0.2 to 1	day ⁻¹
β_3	0.2 to 1	day ⁻¹
α	0.02 to 1	dimensionless
γ^{-1}	2 to 4	days
σ^{-1}	2 to 4	days

COVID-19's lethality on 29 March 2020, according to data released by the Ministry of Health [10], was 3,2%. Because the number of tests for COVID-19 was minimal, especially at the beginning of the pandemic in Brazil, lethality may have been overestimated. Consequently, we considered the value of 1,5% for lethality in the model simulation.

Several simulations were carried out considering three panoramas. The first compares the confirmed cases and deaths reported by the Ministry of Health [11] with the estimates of the model of severe cases and deaths, carried out at two different times, initially without social isolation and later with social isolation. The second panorama is the scenario with and without isolation with the parameters used in panorama 1. The third panorama establishes various forms of isolation.

3.1 Panorama 1

In the first scenario, we estimate the number of severe cases between 4 and 16 March 2020 (13 days) and compare with the data of those infected in Brazil confirmed by the Ministry of Health [11]. The parameters used were $\varepsilon_1\beta_1 = 1$, $\varepsilon_2\beta_2 = 0.5$, $\beta = 0.5$, $\beta_3 = 0.4$, $\alpha = 0.2$, $\gamma^{-1} = \sigma^{-1} = 4$, $\rho_1 = \rho_2 = \rho_3 = 0$, $\varepsilon = \varepsilon_3 = 1$ and $\mu = 0.015$. Furthermore, the initial condition for exposed, infectious and removed individuals were $E_0 = 5$, $I_{01} = 1$, $I_{02} = 3$, $I_{03} = 2$ and $R_0 = 0$.

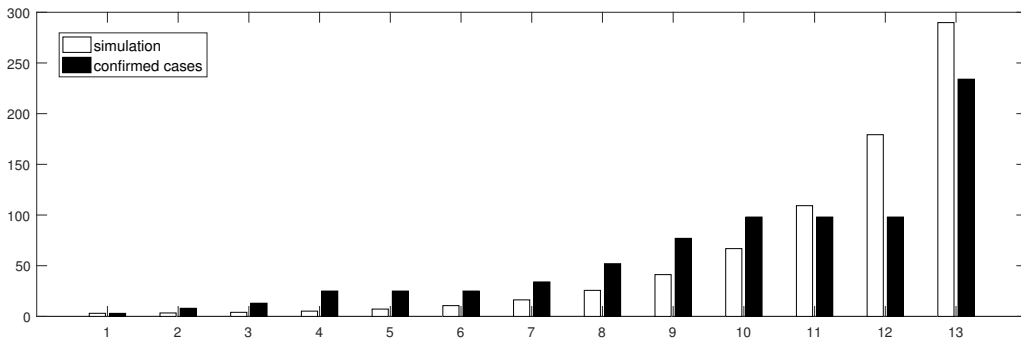


Figure 2: Infectious data by COVID-19 versus simulated values of infectious with severe symptoms in Brazil between 4 and 16 March 2020.

The graph in Figure 2 shows that from 16 March, simulated cases exceeded confirmed cases, which may indicate that cases confirmed by the Ministry of Health are being under-reported.

On 16 March 2020, campaigns for social isolation, protection (using a mask) and hygiene (washing hands with soap and using alcohol in gel) were started by some government officials throughout Brazil in an attempt to control the rapid spread of this disease. Thus, the next simulation considers the isolation in the susceptible subpopulation, estimating the severe symptomatic cases and deaths caused by COVID-19 in Brazil between 17 March and 2 April 2020.

Using the parameters of the previous simulation with the isolation of 70% of children/young people, 40% of adults and 75% of the elderly and considering as an initial condition the solution of the model (2.1) on 16 March, we obtain an estimate for the cases deaths and deaths that are compared with data on infectious and dead by COVID-19 provided by the Ministry of Health [11] (Figure 3).

The data used to generate the simulations shown in the graphs in Figures 2 and 3 are fundamental for the simulations of the scenarios presented in the following subsections, from which we will present the evolution of those infected and the number of deaths by COVID-19 over time, with and without social isolation.

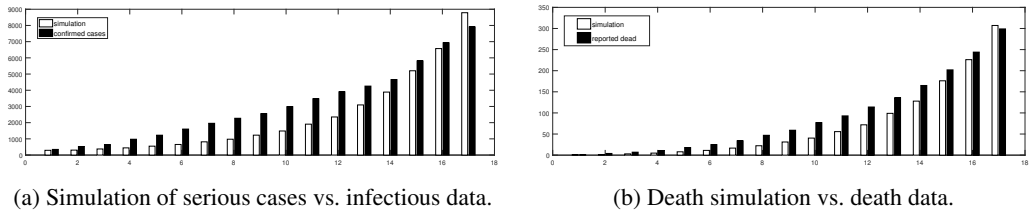


Figure 3: Simulated values of severe symptoms and deaths versus infectious and dead data by COVID-19 in Brazil between March 17th and April 2nd, 2020.

3.2 Panorama 2

In the second scenario, we simulate the dissemination of COVID-19 in Brazil from 4 March to 2 June 2020, equivalent to 90 days, using the same parameters and initial condition that generated the Figure 2, where there is no social isolation.

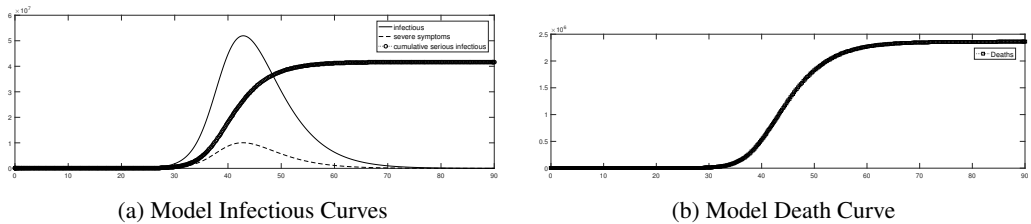


Figure 4: Simulation of infectious and dead by COVID-19 in Brazil from 4 March to 2 June 2020.

The graph in Figure 4 (a) presents three curves, the continuous curve represents the sum of the amount of asymptomatic, mild symptomatic and severe symptomatic infectious, which we will identify as active infectious, reaching the epidemic peak between 14 and 24 April 2020 with approximately 51 million and 947 thousand active infectious, of these 10 million and 40 thousand are severe symptomatic (dashed curve). At the end of 90 days, 41 million and 677 thousand individuals will have contracted the disease and will show severe symptoms (thick curve -o-) and 2 million and 358 thousand will die from COVID-19 (Figure 4 (b)).

The basic reproduction number for this scenario is $\mathcal{R}_0 = 4.19$, which means that on average, an infectious individual infects approximately four people during their infectious period, when exposed to a population of susceptible only [4].

The next scenario depicts the spread of the virus in Brazil from 16 March to 14 August 2020 (150 days), using the parameters and initial condition that generated the graphs in Figure 3, in which there was isolation 70% for children/youth, 75% for elderly and 40% for adults.

The graph in Figure 5 shows that the epidemic peak will occur between 28 May and 7 June 2020 and that there will be 17 million 856 thousand active infectious, being 3 million and 421 thousand

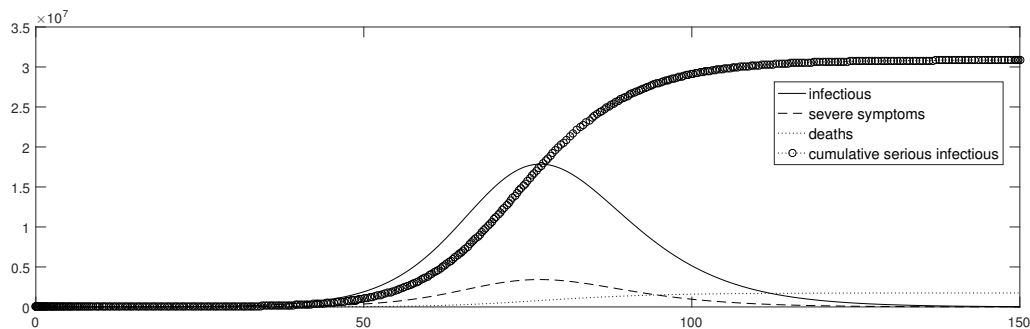


Figure 5: Simulation of infectious diseases and deaths in Brazil from 4 March to 22 November 2020.

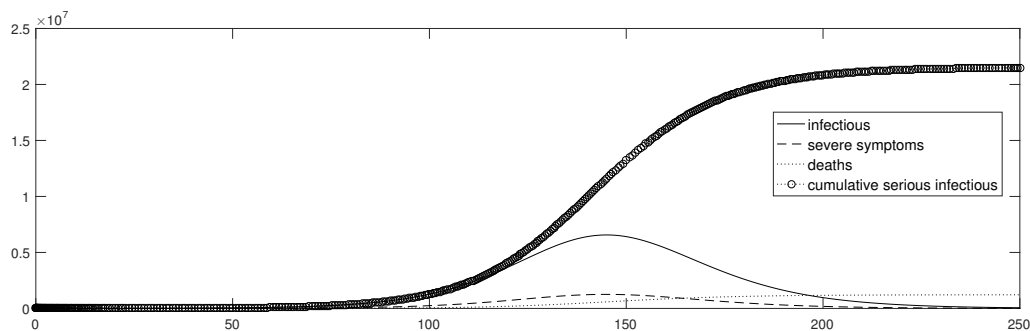


Figure 6: Simulation of infectious diseases and deaths in Brazil from 4 March to 22 November 2020, with 60% exposure of exposed and asymptomatic individuals in contact with susceptible individuals.

severely symptomatic, and at the end of 150 days there will be 30 million and 846,000 serious cases and 1 million and 745 thousand deaths caused by COVID-19. In this simulation the basic reproduction number is $\mathcal{R}_0 = 1.95$.

In practice it is impossible to differentiate between susceptible, exposed and asymptomatic adult individuals, therefore the third scenario in this subsection proposes that asymptomatic infectious and exposed individuals have the same isolation fraction as adult individuals; that is, 40%. Thus, using the same parameters that generated the graphs in Figure 5 and modifying the exposure of exposed and asymptomatic individuals in contact with susceptible individuals to 60%, we obtain the spread of the virus in the Brazilian population in the period from 4 March to 22 November 2020 (250 days), where the basic reproduction number of the disease is $\mathcal{R}_0 = 1.45$.

The graph in Figure 6 shows that the epidemic outbreak will take place approximately on 17 August 2020, reaching 6 million 561 thousand active infectious, of which 1 million and 253 thousand will be severe cases and close to 22 November 2020 21 million and 153 thousand will contract the disease with 1 million and 218,000 deaths by COVID-19.

We can see from the scenarios presented in this subsection that social isolation has an effect both at the peak of the epidemic and at the moment when the peak occurs.

3.3 Panorama 3

In the third scenario, we simulate several variations of social isolation in both the susceptible population and the infectious population, using the same parameters as the first scenario in subsection 3.1.

We start by doing three simulations with the isolation of the susceptible subpopulations in isolation. In the first simulation, we consider that 90% of the susceptible elderly are in social isolation (Figure 7 (a)). In the second simulation, we consider the isolation of 90% of susceptible children/youths (Figure 7 (b)) and then the 90% isolation of susceptible adults (Figure 8).

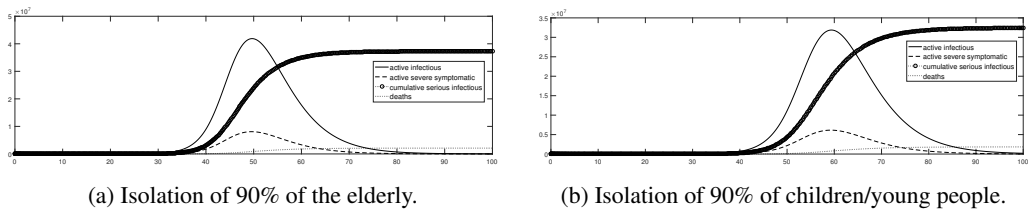


Figure 7: Simulation of the model with social isolation of the elderly (a) and children/youth (b) subpopulation in the period from 4 March to 14 June 2020.

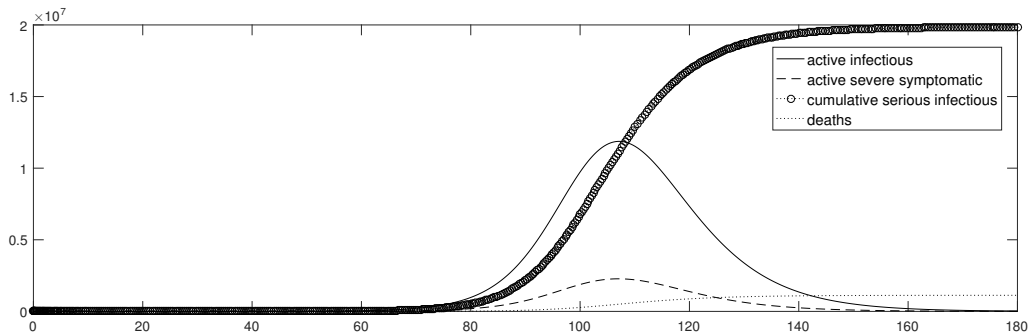
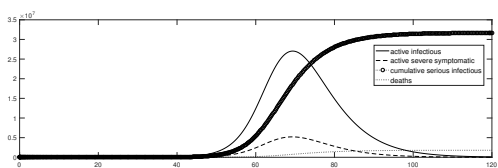


Figure 8: Model simulation with isolation of 90% of adults from 4 March to 4 September 2020.

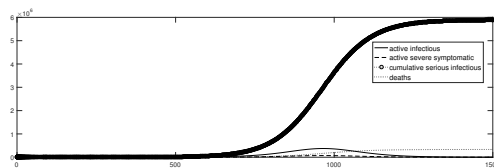
The high dissemination of COVID-19 in the Brazilian population is noticeable in the three graphs in Figures 7 and 8, with the isolation of children/young people being more efficient than that of the elderly and disadvantageous compared to isolation of susceptible adults. Thus, the isolation of susceptible adults generates less contamination, consequently fewer deaths and also delays the emergence of the maximum number of active infection. However, there will still be approximately 19 million and 842,000 infected with severe symptoms and 1 million and 123,000 deaths at the end of 180 days, which is not enough to contain the spread of the disease.

The basic reproduction number for 90% isolation of children/young people is $\mathcal{R}_0 = 3.12$, with 90% isolation of the elderly is $\mathcal{R}_0 = 3.65$ and with 90% isolation of adults is $\mathcal{R}_0 = 2.02$. This indicates that the isolation of only one of the susceptible subpopulations is insufficient to control the spread of the disease.

In the simulation below, we combine the social isolation of the elderly and children/young people to 80%, then add to this combination the isolation of 70% of adults (Figure 9).



(a) Isolation of 80% of the elderly and children/young people.



(b) Isolation of 80% of elderly and children/young people and 70% of adults.

Figure 9: Model simulation starting 4 March 2020 with isolation of susceptible Brazilian subpopulations.

Figure 9 (a) shows that not even a combined high isolation of children/youth and elderly is more effective than isolation of adults only (Figure 8). However, the combined isolation of 80% of elderly and children/young people and 70% of adults (Figure 9 (b)) generated a total of 5 million and 886 thousand infections with severe symptoms and 333 thousand and 180 deaths, with an epidemic peak after 2 and a half years with 373 thousand 818 active infectious, of which 71 thousand 343 infectious with severe symptoms, the basic reproduction number for the two scenarios presented are, respectively, $\mathcal{R}_0 = 2.76$ and $\mathcal{R}_0 = 1.079$.

By increasing the isolation of adults to 75% and keeping the isolation of children/young people and the elderly at 80% in the previous simulation, we get a scenario in which COVID-19 does not invade the population, as can be seen in Figure 10 and the basic reproduction number is $\mathcal{R}_0 = 0.959$.

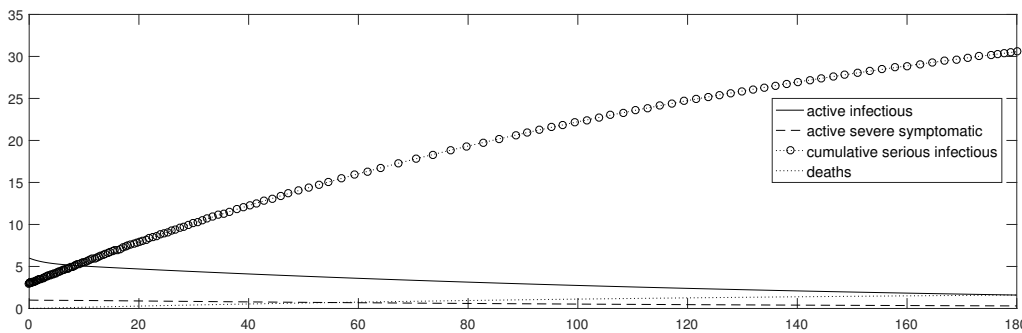


Figure 10: Model simulation starting 4 March 2020 with isolation of 80% from children/young and the elderly and 75% from adults.

Thus, under the considered hypotheses, this result suggests that it is possible to control the dissemination of COVID-19 by combining social isolation by age group of susceptible individuals.

Because exposed and asymptomatic individuals do not present symptoms, we will verify the dissemination of COVID-19 by decreasing the fraction of asymptomatic exposed and infectious individuals that are exposed to direct contact with susceptible individuals. In this way, we can increase the fraction of susceptible adults who can emerge from social isolation.

We can see in Figure 11 that the spread of the virus does not invade the population if we consider the isolation of 80% children/young people and the elderly and 55% from adults, asymptomatic and exposed individuals, being $\mathcal{R}_0 = 0.94$ for this scenario. Thus, this result suggests that the social isolation of those who do not have symptoms (exposed and asymptomatic) favors the control of the spread of the disease.

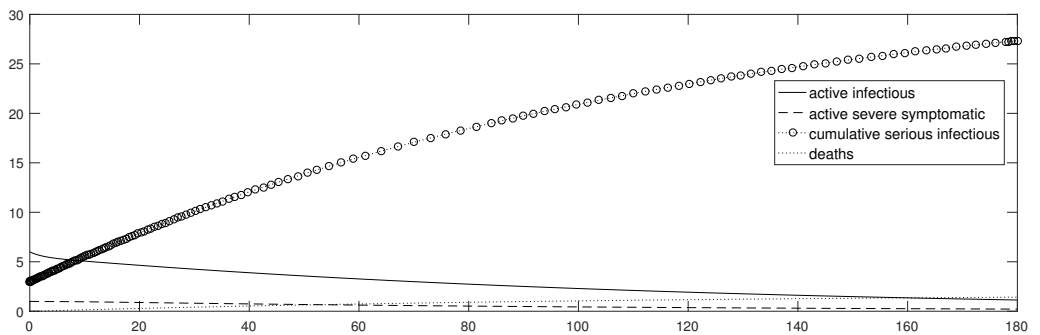


Figure 11: Model simulation starting 4 March 2020 with isolation of 80% from children/youth and elderly and 55% from adults, asymptomatic and exposed individuals.

The last scenario presents the effect of quarantine on the subpopulation of infectious with mild symptoms, those with symptoms such as colds or flu, on the dissemination of COVID-19, with the social isolation of the susceptible, exposed and asymptomatic subpopulations.

Assuming that there was more awareness for the quarantine of infectious with mild symptoms reflecting a reduction of 50% in their transmission power ($\epsilon_2\beta_2$) of COVID-19 and with the social isolation of 80% of children /young and elderly and 50% isolation from adults, asymptomatic and exposed individuals, we obtain a scenario in which the virus does not invade the Brazilian population either (Figure 12) with $\mathcal{R}_0 = 0.92$.

Figure 12 suggests that a combination of measures makes possible the uncontrolled proliferation of the virus in Brazil because the awareness of the Brazilian population to be quarantined if it presents mild symptoms, such as cold or flu, is of paramount importance to control the spread of the disease and the effect of this awareness leads to relaxation of the social isolation of susceptible adults.

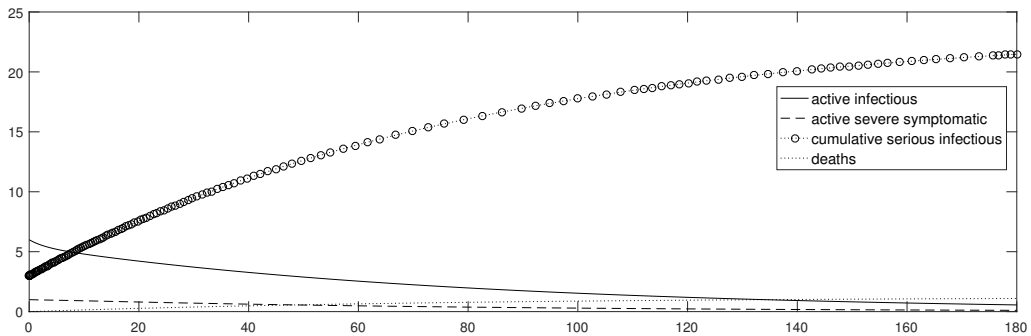


Figure 12: Model simulation on 4 March 2020 with quarantine of infectious individuals with mild symptoms and social isolation.

4 FINAL CONSIDERATIONS

The SEIR compartmental model was adopted to understand the dynamics of the epidemic with diversified isolation and does not assume that there are changes in parameters during the epidemiological process. However, in the real context there is always the possibility of the appearance of new strains of the virus with different strengths of infectivity, and also occasional changes in the composition and sizes of the isolated susceptible groups. These biotic and abiotic factors, which are more frequent after one year, are the main responsible for the wavy behavior of the number of cases. Our study focuses on the first phase of the pandemic when we still do not have viral mutations and/or large behavioral variations of the susceptible ones.

The basic reproduction number of the disease (\mathcal{R}_0) was calculated in section 2 and shows that the isolation by age group of susceptible individuals has a weight given by $\left(\frac{S_i^*}{N}\right)$. In Brazil, the largest fraction is of individuals who are in the range considered adult, so it is evident that the speed of the epidemic is more efficiently slowed down if the susceptible adult subpopulation are the most isolated.

The results presented in subsections 3.1 and 3.2 suggest that the measures adopted in Brazil in March and April 2020 to control the spread of the virus were insufficient to slow down the spread of the disease and the epidemiological scenario worsens without social isolation because the epidemic peak is greater and reached in less time when measures are not taken so that the population respects social isolation.

The results of the 3.3 subsection suggest that the isolation of only one of the susceptible subpopulations is inefficient to control virus propagation, which indicates that vertical isolation is not adequate to contain the proliferation of COVID-19. A more drastic social isolation made up of susceptible subpopulations suggests a smoothing of the spread of COVID-19 in which the disease does not invade the population. In addition, when a portion of latent and asymptomatic individuals are placed in isolation, the results advocate an improvement in the epidemiological scenario in which a larger fraction of adults can be exposed to society without epidemiological evolution

and the effect of awareness for quarantine of infectious individuals with mild symptoms, such as a cold or flu, is of paramount importance for disease control.

Finally, the results suggest that social isolation can be used as an effective tool to control the spread of COVID-19 in Brazil, preventing millions of infections and thousands of deaths when applied vigorously.

REFERENCES

- [1] M.M. Arons, K.M. Hatfield, S.C. Reddy, A. Kimball, A. James, J. Jacob & other. Presymptomatic SARS-CoV-2 infections and transmission in a skilled nursing facility. *New England Journal of Medicine*, **382**(22) (2020), 2081–90.
- [2] COVID-19 Dashboard by the Center for Systems Science and Engineering (CSSE) at Johns Hopkins University (2021). URL <http://coronavirus.jhu.edu/map.html>. Acessado em 09 de maio de 2021.
- [3] Covid-19: veja como cada estado determina o distanciamento social (2020). URL <https://agenciabrasil.ebc.com.br/saude/noticia/2020-04/covid-19-veja-como-cada-estado-determina-o-distanciamento-social>. Acessado em 10 de agosto de 2020.
- [4] P.v.d. Driessche & J. Watmough. Reproduction numbers and sub-threshold endemic equilibria for compartmental models of disease transmission. *Mathematical Biosciences*, **180** (2002), 29–48.
- [5] Y.R. Guo, Q.D. Cao, Z.S. Hong, Y.Y. Tan, S.D. Chen, H.J. Jin, K.S. Tan, D.Y. Wang & Y. Yan. The origin, transmission and clinical therapies on coronavirus disease 2019 (COVID-19) outbreak—an update on the status. *Military Medical Research*, **7**(1) (2020), 1–10.
- [6] Y.H. Jin, L. Cai, Z.S. Cheng, H. Cheng, T. Deng, Y.P. Fan, C. Fang, D. Huang, L.Q. Huang, Q. Huang *et al.* A rapid advice guideline for the diagnosis and treatment of 2019 novel coronavirus (2019-nCoV) infected pneumonia (standard version). *Military Medical Research*, **7**(1) (2020), 4.
- [7] M.U. Kraemer, C.H. Yang, B. Gutierrez, C.H. Wu, B. Klein, D.M. Pigott, L. Du Plessis, N.R. Faria, R. Li, W.P. Hanage *et al.* The effect of human mobility and control measures on the COVID-19 epidemic in China. *Science*, **368**(6490) (2020), 493–497.
- [8] Q. Li, X. Guan, P. Wu, X. Wang, L. Zhou, Y. Tong, R. Ren, K.S. Leung, E.H. Lau, J.Y. Wong *et al.* Early transmission dynamics in Wuhan, China, of novel coronavirus–infected pneumonia. *New England Journal of Medicine*, (2020).
- [9] R. Li, S. Pei, B. Chen, Y. Song, T. Zhang, W. Yang & J. Shaman. Substantial undocumented infection facilitates the rapid dissemination of novel coronavirus (SARS-CoV2). *Science*, (2020).
- [10] Ministério da Saúde. Coronavirus Covid-19 (2020). URL <http://coronavirus.saude.gov.br/>. Acessado em 27 de março de 2020.
- [11] Painel Coronavírus Brasil (2020). URL <http://covid.saude.gov.br/>. Acessado em 06 de abril de 2021.

- [12] Situação da Educação no Brasil (2020). URL <https://pt.unesco.org/fieldoffice/brasil/covid-19-education-Brasil>. Acessado em 10 de agosto de 2020.
- [13] World Health Organization. Coronavirus disease (2020). URL https://www.who.int/health-topics/coronavirus#tab=tab_2. Acessado em 27 de março de 2020.
- [14] World Health Organization. Coronavirus disease (COVID-2019) situation reports (2020). URL <https://www.who.int/emergencies/diseases/novel-coronavirus-2019/situation-reports>. Acessado em 27 de março de 2020.

